Cell. Mol. Life Sci. 65 (2008) 1272 – 1284
1420-682X/08/071272-13
DOI 10.1007/s00018-008-7589-1

Cellular and Molecular Life Sciences

Research Article

Mitochondrial association of alpha-synuclein causes oxidative stress

M. S. Parihar[a], A. Parihar[a], M. Fujita[b], M. Hashimoto[b] and P. Ghafourifar[a,*]

[a] Department of Surgery, Davis Heart and Lung Research Institute, and Institute of Mitochondrial Biology, Ohio State University, 460 West 12th Avenue, Columbus, 43210 OH (USA),
e-mail: Pedram.Ghafourifar@osumc.edu
[b] Laboratory for Chemistry and Metabolism, Tokyo Metropolitan Institute for Neuroscience, Fuchu, Tokyo (Japan)

Received 27 December 2007; received after revision 7 February 2008; accepted 8 February 2008
Online First 25 February 2008

Abstract. α-Synuclein is a neuron-specific protein that contributes to the pathology of Parkinson's disease *via* mitochondria-related mechanisms. The present study investigated possible interaction of α-synuclein with mitochondria and consequences of such interaction. Using SHSY cells overexpressing α-synuclein A53T mutant or wild-type, as well as isolated rat brain mitochondria, the present study shows that α-synuclein localizes at the mitochondrial membrane. In both SHSY cells and isolated mitochondria, interaction of α-synuclein with mitochondria causes release of cytochrome *c,* increase of mitochondrial calcium and nitric oxide, and oxidative modification of mitochondrial components. These findings suggest a pivotal role for mitochondria in oxidative stress and apoptosis induced by α-synuclein.

Keywords. Alpha synuclein, mitochondria, nitric oxide, Parkinson's disease, mitochondrial calcium, cytochrome c, mitochondrial nitric oxide synthase, oxidative stress.

Introduction

α-Synuclein (α-syn) is a major protein component of Lewy bodies and Lewy neuritis that are involved in the pathology of neurodegenerative diseases [1, 2]. Increased aggregation of α-syn into large inclusion bodies and increased accumulation of high molecular weight α-syn plays a significant role in neurotoxicity particularly in dopaminergic neurons of the substantia nigra [3]. The link between α-syn aggregation and disease pathology has been strengthened by the discovery of mutant forms of α-syn, A53T and A30P, that are associated with cases of familial Parkinson's disease [4–8]. However, the exact pathogenic mechanism of those mutants is not fully understood. Overexpression of these α-syn mutants in a cell system provides an opportunity to analyze the molecular pathways underlying normal α-syn biology and its pathogenic consequences. α-Syn associates with membranous structures including mitochondria [9]. Overexpression of α-syn in cells has been suggested to cause elevation of mitochondrial oxidant radicals [10, 11] and mitochondrial structural and functional abnormalities [12–15]. Mitochondria produce NO *via* mitochondrial NO synthase (mtNOS; reviewed in [16]). mtNOS-derived NO readily produces peroxynitrite [16, 17] that induces mitochondrial oxidative stress [17] and release of cytochrome *c* from the organelles [18, 19]. Remarkably, several neurotoxins

* Corresponding author.

involved in neurodegeneration such as amyloid β peptide [20, 21] and mutant huntingtin [22] also induce oxidative stress and apoptosis by releasing cytochrome *c* from mitochondria.

Despite many experimentally tested models, the consequence of α-syn-mitochondrial interaction and molecular mechanism by which α-syn induces neuronal toxicity remains largely elusive. To address this issue, the present study tested α-syn at subcellular levels and examined the effect of α-syn on isolated mitochondria. We show that both A53T mutant and wild-type α-syn are localized at the mitochondria of human neuroblastoma dopaminergic SHSY cells. Overexpression of α-syn A53T mutant or wild-type in SHSY cells, or treatment of isolated rat brain mitochondria with aggregated α-syn causes release of cytochrome *c* from mitochondria, and increase of intramitochondrial ionized calcium ($[Ca^{2+}]_m$) and NO. Our findings introduce a novel mechanism potentially involved in the pathology of α-syn.

Materials and methods

Cell culture

Human dopaminergic neuroblastoma SHSY cells were obtained from ATCC (Manassas, VA). Cells were grown onto poly-D-lysine-coated 12-mm glass coverslips in 24-well plates with DMEM/F-12 (1:1) (Invitrogen) supplemented with 10% fetal bovine serum, 50 U/ml penicillin, and 50 μg/ml streptomycin. All cells were maintained in a humidified 5% CO_2 atmosphere at 37 °C. Viability of the cells was verified by Trypan blue exclusion assay.

α-Syn constructs

To create α-syn A53T expression vector, a two-step PCR strategy was performed as described [23]. Briefly, two sets of primer pairs, sense primer 5'-ATGGATGTATTCATGAAAGGACT-3' (the N-terminal 1–23 oligonucleotide position of α-syn) and antisense primer 5'-CTCAGCCACTGTTGTCACACCATGCAC-3' (antisense sequence of 197–223 oligonucleotide position of α-syn with A53T mutation), and sense primer 5'-GTGCATGGTGTGACAACAGTGGCTGAG-3' (sense sequence 197–223 oligonucleotide position of α-syn with A53T mutation) and antisense primer 5' TTAGGCTTCAGGTTCGTAGTCTTG-3' (the C-terminal 400–423 oligonucleotide position of α-syn) were individually incubated with pCEP4-α-syn as a template in the first PCR reaction. In the second PCR reaction, the PCR products were gel-purified, combined and incubated with the N- and the C-terminal human α-syn primers to synthesize a full-length α-syn A53T cDNA. The resulting PCR products were inserted into mammalian expression vector p-TARGET by TA cloning (Promega Biotech, Madison, WI). To create a wild-type α-syn expression vector, a regular PCR was performed using N- and C-terminal human α-syn primers and subcloned into the p-TARGET, while a self-ligated plasmid of the p-TARGET was used as a control vector. Fidelity of sequences was confirmed for all plasmids.

Transfection

SHSY cells grown on glass coverslips were transfected with α-syn A53T mutant, wild-type, or empty vector at 70–80% confluence using Lipofectamine 2000 (Invitrogen) according to manufacturer's protocol.

Transmission electron microscopy

Subcellular localization of α-syn in cells expressing A53T mutant was tested by immuno-gold electron microscopy. SHSY cells were grown on 22-mm coverslips in six-well plates. At 48 h after transfection, cells were fixed in 4% paraformaldehyde and 0.04% glutaraldehyde in 0.1 M PBS (pH 7.4) for 3 h at 4 °C. Cells were post-fixed with 0.05% osmium tetroxide 15 min at 4 °C, dehydrated with graded acetone and embedded in Spurr resin (Agar Scientific, Stansted, Essex, UK). Ultrathin sections (80 nm) were cut following polymerization using ultramicrotome (Leica Microsystems). Sections were permeabilized on Formvar-coated nickel grids with aqueous 10% hydrogen peroxide for 15 min, washed three times for 5 min each in D-PBS (Gibco), and exposed for 30 min to 5% heat-treated normal goat serum (NGS) in PBS (Electron microscopy science, Hatfield, PA). Sections were incubated overnight at 4 °C with primary α-syn antibody (H3C; 1:100 dilution) followed by incubation in gold-labeled rabbit anti-mouse IgG (Electron microscopy science). Sections were washed twice for 5 min each with 5% NGS in PBS, then further washed in D-PBS twice 10 min each. Sections were fixed in 2% glutaraldehyde, and washed three times in D-PBS and twice in H_2O. Samples were stained with 2% uranyl acetate and lead citrate for 5 min and air dried. Electron micrographs were taken using electron microscope (Tecnai G2, Hillsboro, OR) operated at 100 kV.

Immunofluorescence staining

To determine subcellular distribution of α-syn and cytochrome *c,* cells were loaded with the mitochondrial marker mitotracker red (CM-H_2Xros; Molecular Probes; 500 nM) in DMEM/F-12 medium under 5% CO_2 at 37 °C for 30 min, washed three times with PBS, and fixed in freshly prepared 4% paraformaldehyde for 20 min at 4 °C. After three washes in TBS, the

samples were immunostained overnight with monoclonal antibody against α-syn (H3C; 1:500 dilution) or anti–cytochrome *c* antibody (BD Biosciences Pharmingen, 1:200 dilution) followed by 60-min incubation with an anti-mouse Alexa 488-conjugated secondary antibody (Molecular Probes: 1:200 dilution).

Loading with fluorescent dyes and performing confocal imaging

To measure $[Ca^{2+}]_m$, cells were loaded with rhod-2AM (Molecular Probes; 5 μM) simultaneously with mitotracker green FM (200 nM) in DMEM/F-12 medium under 5% CO_2 at 37 °C for 45 min. Probed cells were permeabilized with digitonin (10 μM) to eliminate the cytosolic fraction of rhod-2 [24]. As a positive control, $[Ca^{2+}]_m$ was elevated by treating cells with ionomycin (10 μM) for 30 min before loading with fluorescent dye [25]. At the end of each measurement, carbonyl-cyanide-*p*-trifluoro-methoxy-phenylhydrazone (FCCP) (5 μM) was used to deplete $[Ca^{2+}]_m$ by collapsing mitochondrial transmembrane potential ($\Delta\psi$). To measure mitochondrial NO, cells were incubated with mitotracker red (200 nM) and membrane permeable NO probe, 4,5-diaminofluorescein diacetate (DAF-2DA; 5 μM; Calbiochem) under 5% CO_2 at 37 °C for 20 min [24]. Probed cells were permeabilized with digitonin (10 μM) to eliminate the cytosolic fraction of DAF-2.

Fluorescent image acquisition and processing

The coverslips containing probed cells were washed twice with low fluorescence DMEM. Image acquisition was performed using a Zeiss confocal microscope equipped with LSM 5 software with a 63× water objective. Fluorescence measurement was performed using multichannel detection of excitation with the 488-nm line of an argon laser and the 543- and 633-nm lines of HeNe1 and HeNe2 at room temperature. Fluorescence mitotracker red and rhod-2 images were acquired using 543-nm excitation and 579-nm emission. Fluorescence DAF-2, mitotracker green and Alexa 488, were acquired using 488-nm excitation and 516-nm emission. Images were acquired at 12-bit resolution by taking a single z-stack 1-μm steps. Fluorescence intensity was quantitated using ImageJ (NIH).

Isolation and purification of rat brain mitochondria and microsomes

Isolation and purification of brain mitochondria was performed as described [26]. Brains were removed, washed, and homogenized in Medium A [320 mM sucrose, 1 mM potassium EDTA, 0.1% fatty acid-free BSA (FAF-BSA), 10 mM Tris-HCl pH 7.40]. The homogenate was centrifuged at 1100 *g* for 10 min and the supernatant was re-centrifuged at 19000 *g* for 20 min to obtain crude mitochondrial fraction. The pellet was resuspended in Medium A, laid on 6% Ficoll solution, and centrifuged at 19000 *g* for 30 min. Supernatant and the fluffy layer above the mitochondria pellet were discarded. Each 10 mg of the brown pellet was resuspended in 70 mg Purification Medium [2.56 g 20% (w/w) dextran T500, 1.28 g 40% (w/w) polyethylene glycol (PEG) 4000, 2.24 g 1 M sorbitol, 70 mg 10 mM potassium EDTA, 700 mg 1% FAF-BSA, 200 mg 200 mM potassium phosphate pH 7.80, and H_2O to 7.00 g) and centrifuged at 600 *g* for 2 min in a swing-bucket centrifuge. The upper phase was discarded, 300 μl Washing Medium [96 mg 20% (w/w) dextran T500, 480 mg 40% (w/w) PEG 4000, 960 mg 1 M sorbitol, 75 mg 200 mM potassium phosphate pH 7.80, 30 mg 10 mM potassium EDTA, 300 mg 1% FAF-BSA, and H_2O to 3.00 g) was added to the lower part, mixed and centrifuged at 600 *g* for 2 min. The upper part was discarded and the lower part was mixed with 3 ml Medium B (320 mM sorbitol, 1 mM potassium EDTA, 0.1% FAF-BSA, 5 mM potassium phosphate pH 7.80). The suspension was centrifuged at 19000 *g* for 20 min, and the mitochondrial pellet was collected. The supernatant was centrifuged for 1 h at 100000 *g* to yield the microsomal pellet as described [27]. All steps were carried out at 4 °C. Purity of the isolated mitochondria was assessed by measuring cytochrome *a* using an $\varepsilon_{605-630\,nm}$ 12 $mM^{-1}\,cm^{-1}$ as described [28], and detecting cytochrome oxidase using Western blot. Possible contamination of the isolated mitochondria with cytoplasm was ruled out by lack of detectable cytoplasmic marker Cu/Zn superoxide (Cu/Zn SOD), as determined by Western blot. Only mitochondria with less than 5% impurity were used.

Preparation of mitochondria and cytoplasm of SHSY cells

Mitochondria and cytoplasm were isolated from SHSY cells as described [29]. Briefly, cells were homogenized in lysis buffer (250 mM sucrose, 10 mM Tris-HCl pH 7.40, 1 mM EDTA, 10 μg/ml leupeptin, 40 U/ml aprotinin, 10 μg/ml pepstatin A, 0.2 mM phenylmethylsulfonyl fluoride), centrifuged at 1500 *g* for 10 min, and the supernatant was kept on ice. The pellet was re-homogenized with 3 ml isolation buffer (320 mM sucrose, 1 mM potassium EDTA, 10 mM Tris-HCl pH 7.4), and the homogenate was centrifuged at 1500 *g* for 5 min. Both supernatants were pooled and centrifuged at 1500 *g* for 10 min. The supernatant of this centrifugation was further centrifuged at 17000 *g* for 10 min. The pellet, *i.e.*, the mitochondrial fraction, was resuspended in 200 μl isolation buffer to obtain about 4 mg mitochondrial

protein/ml. All steps were carried out at 4 °C. Purity of the mitochondrial preparation was tested by measuring cytochrome *a* as described above. Intactness of mitochondria was verified by measuring the transmembrane potential that was rapidly collapsed by the uncoupler FCCP.

Treatment of isolated mitochondria or microsomes with α-syn

α-Syn (rPeptide, Bogart, GA, [30]) was aggregated by incubating in sterilized phosphate-buffered saline at 37 °C for 7 days [31]. Aggregation of α-syn was confirmed by gel electrophoresis. Isolated brain mitochondria were pre-incubated 30 min on ice in the absence or presence of mtNOS inhibitor L-N^G-monomethyl arginine (L-NMMA, 100 μM, [18, 19, 32]) followed by treatment with aggregated α-syn (1 μg/ml; [9]) for 30 min at room temperature. Control mitochondria were treated with equal amount of unaggregated α-syn. Binding of α-syn to microsomes was tested as above, except microsomes were used in place of mitochondria. For Western blot analyses, a protease inhibitor cocktail containing aprotinin, pepstatin A, phenylmethanesulfonyl fluoride, and leupeptin (10 μM each, [17]) was present in the incubation medium.

Protein tyrosine nitration, Cu/Zn SOD, cytochrome oxidase, and cytochrome *c* immunoblotting

Samples were immunoblotted against monoclonal anti-nitrotyrosine antibody (Alexis, San Diego, CA) for detection of protein tyrosine nitration, anti-Cu/Zn SOD for detection of Cu/Zn SOD (Calbiochem), or anti-cytochrome oxidase (anti-oxphos complex IV subunit VIc, mouse IgG; Molecular Probes, Eugene, OR) for detection of cytochrome oxidase. To detect cytochrome *c* release, samples were centrifuged at 10000 *g* for 10 min and the supernatants were re-centrifuged at 100000 *g* for 20 min. The second supernatant and pellet were immunoblotted against monoclonal anti-cytochrome *c* antibody (eBiosciences, San Diego, CA).

Binding of α-syn to isolated mitochondria or microsomes

Binding of α-syn to brain mitochondria was tested by immunoblotting the pellet and supernatant of mitochondria treated with aggregated or unaggregated α-syn as described [9]. Mitochondria or microsomes were treated with α-syn as described under *Treatment* and centrifuged at 10000 *g* for 5 min. The supernatant containing unbound α-syn was collected. The pellet was washed twice with isolation buffer followed by centrifugation at 10000 *g* for 5 min and the pellet of second centrifugation was collected to test for bound α-syn. Samples were immunoblotted with monoclonal antibody against α-syn (H3C; 1:5000, courtesy of Dr. Julia M. George, University of Illinois at Urbana-Champaign, IL).

Proteinase K treatment

Mitochondria were treated with α-syn as described under *Treatment.* Proteinase K was added to the mitochondria treated with α-syn at a final concentration of 50 μg/ml and samples were incubated for 25 min at 0 °C [33]. Protease inhibitor cocktail containing aprotinin, pepstatin A, phenylmethanesulfonyl fluoride, and leupeptin (10 μM each) was then added to α-syn-treated samples and further incubated for 10 min at 0 °C. Samples were centrifuged at 10000 *g* for 10 min. Supernatant and pellet were separated and immunoblotted against α-syn monoclonal antibody.

Permeability transition and lipid peroxidation of isolated mitochondria

Permeability transition (permeability transition pore, PTP) was detected at 540 nm as described [34]. Lipid peroxidation (LPO) was measured by thiobarbituric acid assay as described [17, 28].

Nitric oxide synthase activity of isolated mitochondria

Nitric oxide synthase activity was determined by the following assays.

Oxyhemoglobin (oxyHb) assay. Broken mitochondria were prepared from α-syn-treated mitochondria by freeze-thawing as described [18, 28]. mtNOS activity was detected at 401–420 nm in the presence of oxyHb (4 μM) using an extinction coefficient of 100 $mM^{-1}\,cm^{-1}$ [28].

Citrulline radioassay. Mitochondria were treated as under *Treatment*; the incubation medium was supplemented with [L-^{3}H]arginine (30000–50000 cpm). Radio-labeled L-citrulline was measured as described [18, 28].

Chemiluminescence sssay. Treated mitochondria (100 μg) were injected into the purge vessel containing vanadium chloride (0.8% in 1 M HCl) thermostated at 93 °C, and NO was measured using a chemiluminescence analyzer (Sievers 280i, General Electric, Boulder, CO) as described [18].

Determination of $[Ca^{2+}]_m$

Determination of $[Ca^{2+}]_m$ was performed using the highly sensitive dual-wavelength excitation fluorometric assay recently established in our lab [18, 19, 35]. Briefly, isolated mitochondria were loaded with fura-

2/acetoxymethylester (10 μM; 15 min on ice and washed twice with cold buffer), excited from 320 to 400 nm and emission was collected at 510 nm. A clear peak and a sharp isosbestic point were detected at 352 and 362 nm, respectively. $[Ca^{2+}]_m$ was measured by exciting loaded mitochondria at dual-wavelengths of peak minus isosbestic point (352–362 nm) and detecting the emission at 510 nm.

Statistical analysis

Barograms are mean ± SEM. Differences were tested by unpaired Student's *t*-test and considered significant at $p<0.05$. All computations were performed using PlotiT (Scientific Programming, Hazlet, MI).

Results

α-Syn localization in mitochondria

Considering the significance of α-syn in neuronal cell death and the pivotal role of mitochondria in this process, the present study investigated the importance of mitochondria in α-syn-induced neurotoxicity. SHSY cells were transfected with α-syn A53T (A53T) mutant or wild-type and subcellular localization of α-syn was tested using confocal microscopy. Figure 1A shows intense co-localization of the green fluorescence of α-syn with red fluorescence of mitotracker red in both cells overexpressing α-syn A53T or wild type. Control cells show that basal endogenous α-syn distributed in the cytoplasm slightly co-localize with the mitochondria. Figure 1B shows quantitative fluorescent intensity of α-syn in mitochondria of cells expressing A53T or wild-type α-syn that is significantly higher than that of control. Mitochondrial localization of α-syn was confirmed by immuno-gold electron transmission microscopy. Figures 1C and D show localization of α-syn in the mitochondria of wild-type (Fig. 1C) and A53T (Fig. 1D) overexpressing cells that confirm findings presented in Figure 1A. Few immuno-gold particles were also found in the cytoplasm.

α-Syn releases cytochrome *c* from mitochondria

Release of cytochrome *c* from mitochondria is a key event inducing apoptosis in many cells including neurons. The present study detected cytochrome *c* using confocal microscopy and Western blot. Figure 2A shows that, in control cells, cytochrome *c* signal was punctated and co-localized with mitochondria, whereas in cells overexpressing wild-type or A53T cytochrome *c* was scattered in the cytoplasm. This finding indicates release of cytochrome *c* from the mitochondria of cells overexpressing wild-type or A53T α-syn. Figure 2B supports these findings by showing release of cytochrome *c* from the mitochondria of α-syn A53T and wild-type overexpressed cells, as determined by Western blot.

α-Syn increases intramitochondrial NO

Elevated mitochondrial NO causes cytochrome *c* release in variety of cells [17–19]. Thus, we tested mitochondrial NO in cells overexpressing α-syn. Figures 3A and B show increased mitochondrial NO in cells overexpressing wild-type or A53T α-syn, compared to control cells.

α-Syn increases $[Ca^{2+}]_m$

Mitochondrial NO formation is sensitive to $[Ca^{2+}]_m$. Therefore, we tested whether expression of α-syn A53T or wild type is associated with changes in $[Ca^{2+}]_m$. Figures 4A and B show higher $[Ca^{2+}]_m$ in wild-type and A53T α-syn-expressing cells, compared to control cells. As shown in Figures 4A and B, ionomycin that was used as a positive control increased $[Ca^{2+}]_m$, and FCCP that depletes mitochondria of $[Ca^{2+}]_m$ decreased the $[Ca^{2+}]_m$.

The above findings (Figs. 1–4) show localization of α-syn in mitochondria of SHSY cells overexpressing wild-type or A53T α-syn causing cytochrome *c* release and increased mitochondrial NO and $[Ca^{2+}]_m$. To confirm these results, we tested effects of α-syn on isolated rat brain mitochondria.

Aggregation of α-syn and its effects on isolated rat brain mitochondria

First, we verified the purity of our mitochondrial preparation using mitochondrial marker cytochrome oxidase, and cytoplasmic marker Cu/Zn SOD. Figures 5A and B show that mitochondria contained cytochrome oxidase, whereas no detectable Cu/Zn SOD was observed. These findings validate the purity of mitochondrial preparation and suggest negligible contamination of mitochondria with cytoplasmic components. Next we tested aggregation of α-syn peptide. Figure 5C shows un-aggregated α-syn at approximately 19 kDa consistent with the monomeric size and oligomers of aggregated α-syn. Next, we tested binding of α-syn to mitochondria by incubating isolated mitochondria with aggregated or unaggregated α-syn. Figure 5D shows that mitochondria pellet contained significant amount of oligomer α-syn, indicating binding of α-syn oligomers to mitochondrial membrane. However, most of the α-syn monomer was found in supernatants of those samples. To study the nature of α-syn association with mitochondria, α-syn-treated mitochondria were incubated with proteinase K. Proteinase K removes proteins that unspecifically associate with mitochondrial membranes [33]. Figure 5E shows that aggregated α-syn

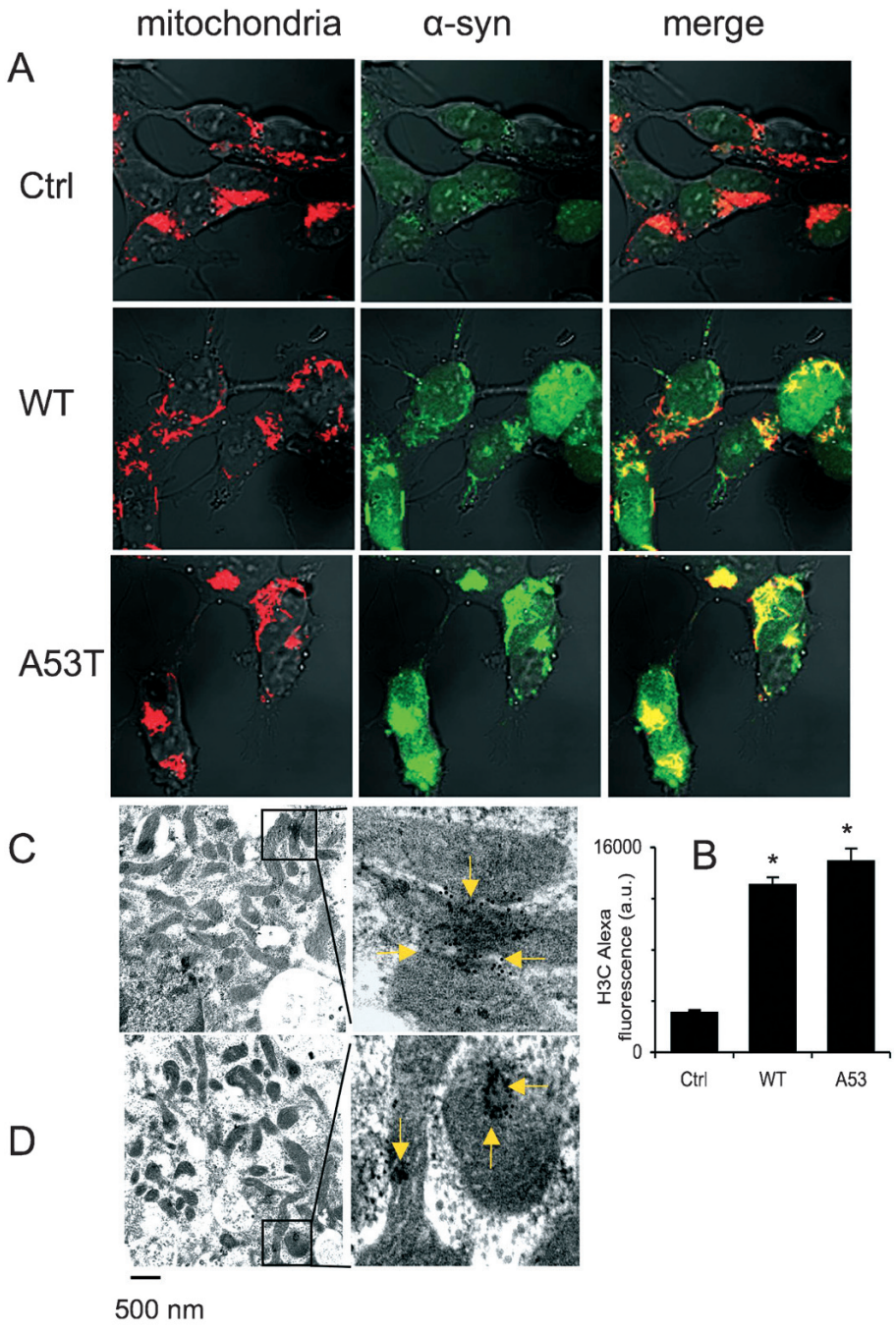

Figure 1. Mitochondrial localization of α-synuclein (α-syn). (*A*) Overexpressing α-syn A53T (A53T), wild-type (WT) and control cells (Ctrl) were loaded with mitotracker red (mitochondria) and immunostained for α-syn using monoclonal α-syn antibody (α-syn). Fluorescence was detected by confocal microscopy. The α-syn immunoreactivity is shown in green, mitochondria staining in red, and the merge image (merge) is yellow for overlapping red and green signals. (*B*) Quantitation of fluorescence intensity of α-syn immunoreactivity in the mitochondria of A53T (A53T), wild-type (WT) and control (Ctrl) cells. (*C*) Immuno-gold electron microscopically localization of α-syn in the mitochondria and cytoplasm of wild-type α-syn-overexpressing cells. (*D*) Immuno-gold electron microscopically localization of α-syn in the mitochondria and cytoplasm of A53T α-syn-overexpressing cells. Inset show zoomed area of mitochondria where immuno-gold labeled particles are localized and shown by arrows.

largely remained in mitochondria pellet even after proteinase K treatment. Figure 5F shows lack of association of aggregated α-syn with microsomes.

To confirm data of cell experiments and to test whether release of cytochrome *c* was a result of direct interaction of aggregated α-syn with mitochondria, release of cytochrome *c* was tested in mitochondria treated with aggregated α-syn. Figure 6A shows that aggregated α-syn induces cytochrome *c* release from isolated mitochondria. To examine the role of mitochondrial NO in cytochrome *c* release, mitochondrial NO formation was inhibited in samples treated with aggregated α-syn. As shown in Figure 6A, L-NMMA dramatically prevented α-syn-induced cytochrome *c* release. Protein tyrosine nitration is a reliable biomarker of NO-dependent oxidative stress and mitochondria are critical sources and targets of nitrating species. Figure 6B shows mitochondrial protein tyrosine nitration. As shown, α-syn increases tyrosine nitration of several mitochondrial proteins, and that this was dramatically prevented when NO was inhibited. Tyrosine nitrated BSA was used as a positive

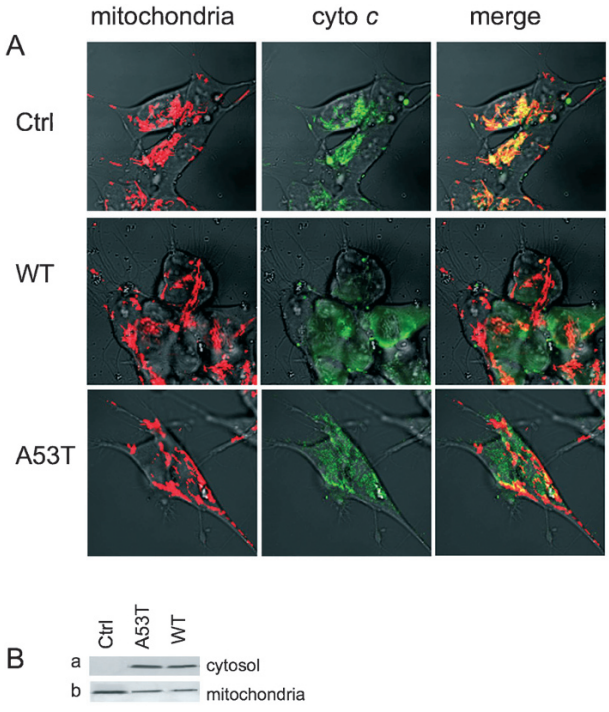

Figure 2. α-Syn wild-type and A53T induces cytochrome *c* release. (*A*) Overexpressing α-syn A53T (A53T), wild-type (WT) and control cells (Ctrl) were loaded with mitotracker red (mitochondria) and immunostained for cytochrome *c* (cyto *c*) using monoclonal anti-cytochrome *c* antibody and Alexa 488. Merge shows mitochondria and cyto *c* overlay pictures. (*B*) Using Western blot analysis, panel *a* shows cytochrome *c* released into the cytoplasm of A53T and WT SHSY cells, and panel *b* shows cytochrome *c* remaining in the mitochondrial fraction of those cells.

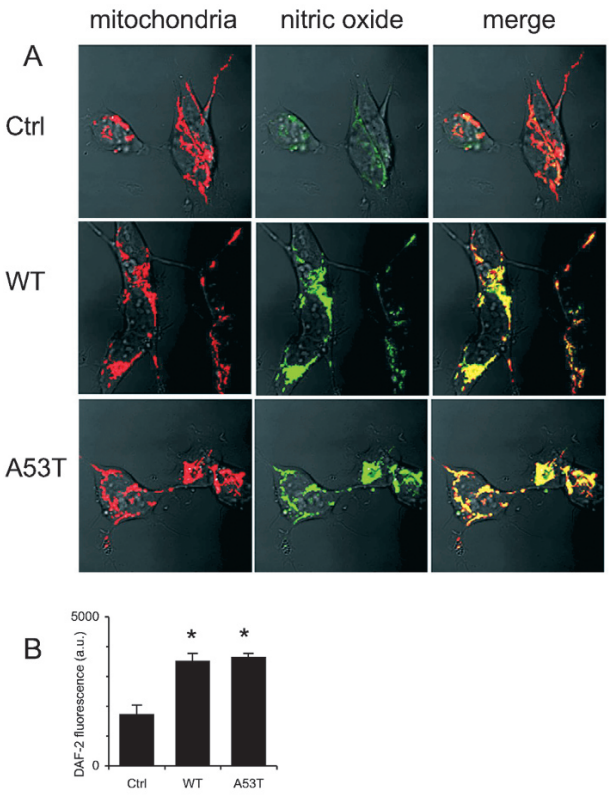

Figure 3. α-Syn wild-type and A53T increases mitochondrial NO. (*A*) NO production in overexpressing α-syn A53T (A53T), wild-type (WT) and control (Ctrl) cells as detected by mitotracker red (mitochondria) and NO fluorescence probe DAF-2DA (nitric oxide). (*B*) Bars show mean ± SE fluorescence intensity of mitochondria (n=200) from at least four to six cells from three to five coverslips.

control, and cytochrome oxidase was used as loading control. Next, the effect of α-syn on LPO and PTP as oxidative stress markers was tested. Figure 6C shows that treatment of mitochondria with aggregated α-syn elevated mitochondrial LPO, and this was prevented by L-NMMA. Figure 6D shows that α-syn caused PTP opening and that removing mitochondrial Ca^{2+} prevented α-syn-induced PTP.

Since effect of α-syn on releasing cytochrome *c*, and increasing LPO and tyrosine nitration were prevented when mtNOS was inhibited, we tested whether α-syn stimulates mtNOS activity. Figures 7A–C show that aggregated α-syn increased mitochondrial NO as determined by all three assays, and that L-NMMA prevented this effect of α-syn. Elevation of $[Ca^{2+}]_m$ stimulates mitochondrial NO formation, elevates LPO, and induces PTP opening [17–19, 34]. Therefore, we tested effect of α-syn on $[Ca^{2+}]_m$. Figure 7D shows that α-syn increased $[Ca^{2+}]_m$ and that L-NMMA did not attenuate increase of $[Ca^{2+}]_m$.

Discussion

α-Syn plays a significant role in the pathology of Parkinson's disease. Aggregation of α-syn and increased oxidative stress in dopaminergic neurons are main hallmarks of Parkinson's disease [4, 5]. Both recombinant α-syn [9] and α-syn mutant A53T interact with membranes [36] and binding of α-syn to membranes is necessary for α-syn toxicity [37]. Mitochondria are membranous organelles that have been suggested as cellular targets for α-syn neurotoxicity [38]. However, the significance of mitochondria in cell death caused by α-syn is not well understood. The present study used two experimental models, human dopaminergic neuroblastoma SHSY cells and isolated rat brain mitochondria, and investigated mitochondrial localization of α-syn and consequences of α-syn-mitochondrial interaction.

First, we tested subcellular localization of α-syn. Figures 1A and B show endogenous α-syn distributed in the cytoplasm of control cells and very minimal α-syn was detected in the mitochondria. Cells over-

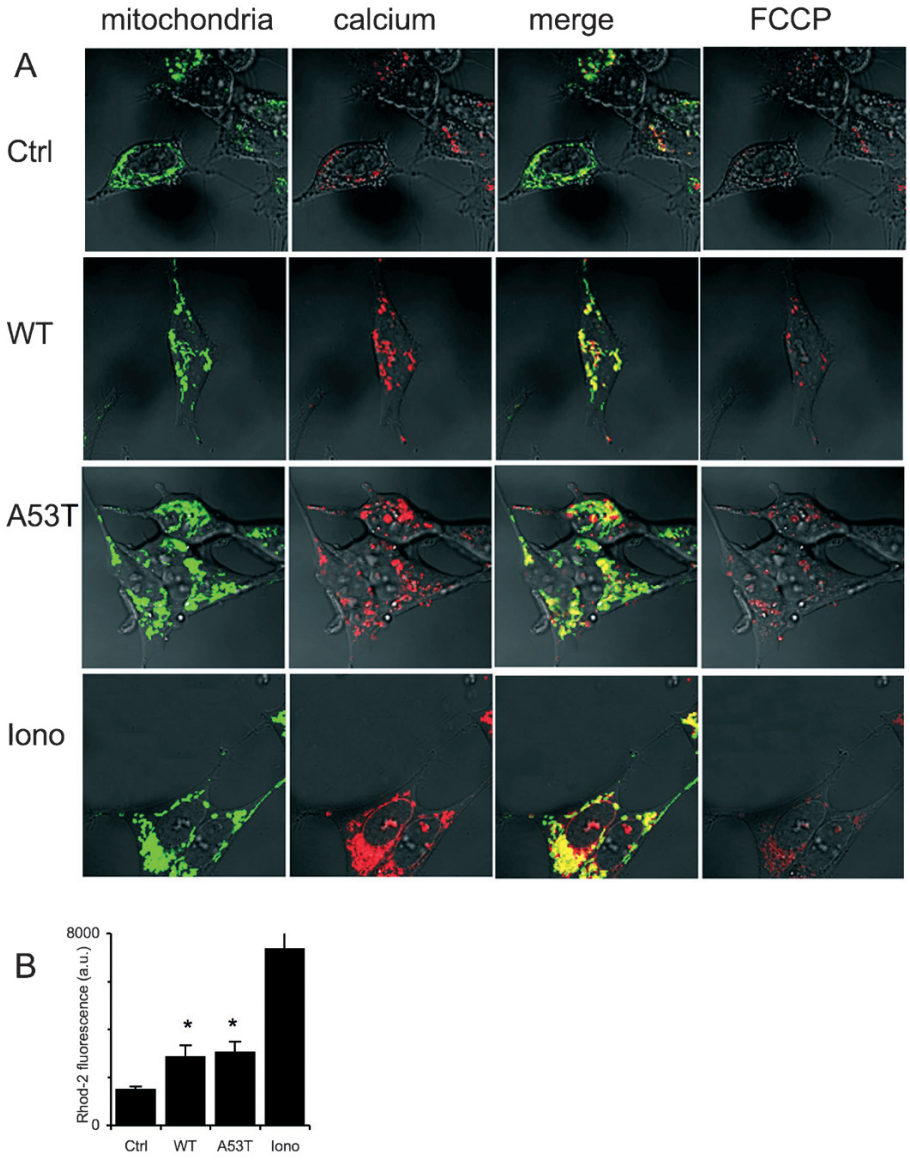

Figure 4. α-Syn wild-type and A53T increases mitochondrial $[Ca^{2+}]_m$. (*A*) α-Syn A53T overexpressing (A53T), wild-type (WT), or control (Ctrl) cells were co-loaded with mitotracker green (mitochondria) and rhod-2AM (calcium). Confocal images of green mitochondria fluorescence and red calcium fluorescence were collected. Merge shows mitochondria and calcium images overlaid. FCCP was added at the end of each imaging as a negative control. Cells were treated with ionomycin (Iono) used as positive control. (*B*) Bars show mean ± SE fluorescence intensity of mitochondria (n=200) from at least four to six cells from three to five coverslips.

expressing wild-type or A53T mutant α-syn, however, exhibited immunoreactivity associated with most of their mitochondria. To confirm association of wild-type or A53T α-syn with mitochondria observed by confocal microscopy, we performed immuno-gold electron microscopy. Figures 1C and D show that α-syn wild-type or A53T were, indeed, localized in the mitochondria of wild-type or A53T mutant overexpressing cells. Some immuno-gold spots were also distributed in the cytoplasm, which is consistent with cytoplasmic α-syn in wild-type or A53T cells (Fig. 1A). Using transgenic mice expressing human wild-type or familial Parkinson's disease-linked A53T or A30P mutant α-syn, electron microscopic studies showed α-syn cross-reacting immuno-gold spots co-localize with degenerating mitochondria deposited onto cytoplasmic inclusions [39]. Very recently, one study used electron microscopy and suggested that in dopaminergic neurons of the mouse substantia nigra pars compacta, α-syn is located at mitochondrial membrane [40]. Our study clearly indicates that both wild-type and A53T α-syn are located at mitochondrial membrane of overexpressing cells.

We next determined the factors render neuronal cells sensitive to α-syn toxicity. It is evident that aggregation of wild-type and A53T is associated with enhanced cell death [41]. We tested whether overexpression of wild-type or A53T α-syn induce cytochrome *c* release from mitochondria, which is a key pro-apoptotic event in most forms of apoptosis. Figure 2A shows that expression of wild-type or mutant A53T α-syn induced cytochrome *c* release from mitochondria of SHSY cells. As shown in this figure, cytochrome *c* was localized within the mito-

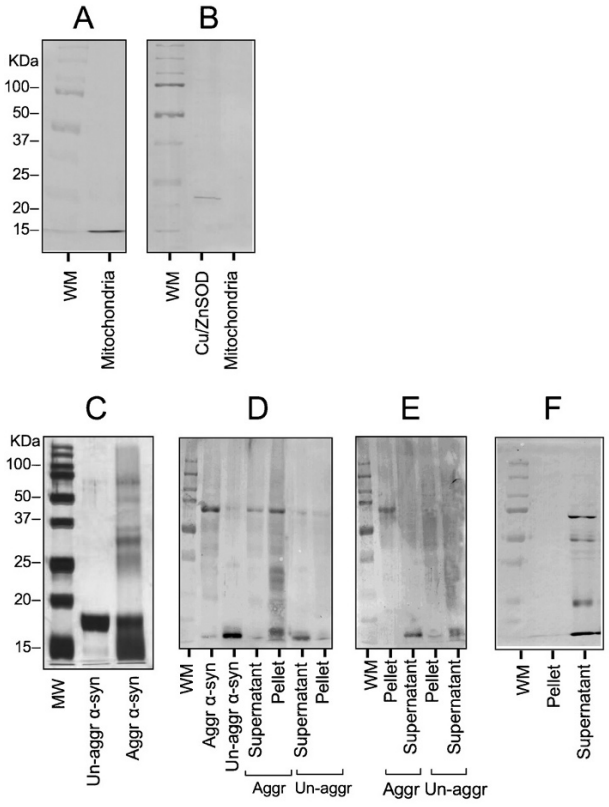

Figure 5. Aggregation and mitochondrial binding of α-syn. (*A*) Immunoblot using anti-cytochrome oxidase antibody shows that mitochondrial preparation contains cytochrome oxidase. (*B*) Immunoblot using anti-Cu/Zn superoxide dismutase antibody (Cu/Zn SOD) shows that mitochondrial preparation is not contaminated with cytoplasm. (*C*) Silver-stained SDS-PAGE showing unaggregated α-syn (un-aggr α-syn) and aggregated α-syn (aggr α-syn). Lane marked MW shows molecular mass in kDa. Un-aggregated α-syn migrated at about 19 kDa, consistent with monomeric size. Aggregated α-syn showed both low and high molecular mass. (*D*) Immunoblot with monoclonal anti-α-syn antibody showing pellet and supernatant of mitochondria incubated with aggregated or un-aggregated α-syn. (*E*) Aggregated α-syn or un-aggregated α-syn treated mitochondria were incubated with proteinase K. Supernatant and pellet were analyzed by Western blot. (*F*) Immunoblot using monoclonal anti-α-syn antibody showing pellet and supernatant of microsomes incubated with aggregated α-syn.

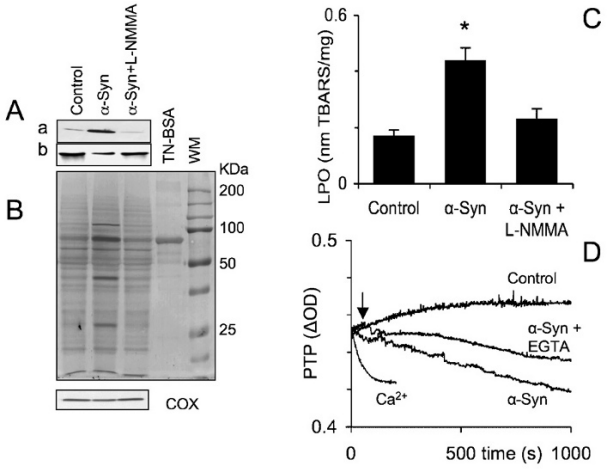

Figure 6. Effect of α-syn on isolated brain mitochondria. Mitochondria were treated with un-aggregated α-syn (control), aggregated α-syn (α-syn), or aggregated α-syn after pretreatment of mitochondria with L-NMMA (α-syn + L-NMMA). (*A*) Cytochrome *c* released from the mitochondria into the supernatant (a) and cytochrome *c* in the pellet (b). (*B*) Tyrosine nitration of mitochondrial proteins. Tyrosine nitrated BSA (TN-BSA) was used as positive control. Molecular weight marker (WM) is shown in kDa. Cytochrome oxidase (COX) served as loading control. (*C*) Lipid peroxidation (LPO) of mitochondria expressed as nmol thiobarbituric acid reactive substance (TBARS) per mg mitochondrial protein. (*D*) Induction of mitochondrial permeability transition (PTP) was measured and expressed as ΔOD at 540 nm. Mitochondria were treated with aggregated α-syn (α-syn) or un-aggregated α-syn (control) in the absence or presence of EGTA. Ca^{2+} indicates when PTP was induced by loading mitochondria with 40 μM Ca^{2+}. Arrow indicates addition of Ca^{2+}. $^*p<0.05$ compared with the control; $n\geq 6$.

chondria of control cells, whereas cytochrome *c* was diffused in the cytoplasm of cells expressing wild-type or A53T α-syn, indicating cytochrome *c* was released from the mitochondria of those cells. In support of these findings, Figure 2B used Western blot analysis and shows that cytochrome c was released from the mitochondria of cells expressing A53T and WT α-syn. Studies conducted in PC12 cell lines [36] and primary cortical neurons [42] suggested that α-syn A53T interacts with mitochondria and that α-syn might induce cytochrome *c* release [36, 39, 43]. Our findings clearly show that overexpression of α-syn causes cytochrome c release, which could well serve mechanism underlying pro-apoptotic properties of α-syn.

Altered cellular calcium homeostasis along with elevated cellular NOS activity contributes to the apoptosis of dopaminergic neurons in Parkinson's disease [44, 45]. The present study shows that overexpression of wild-type or A53T α-syn caused a dramatic increase in mitochondrial NO compared to control cells (Fig. 3). These novel findings strongly suggest that α-syn wild-type or A53T stimulate mtNOS in human dopaminergic neurons.

Our previous studies showed that intramitochondrial NO is increased upon increase in $[Ca^{2+}]_m$ [17–19, 35], therefore we tested changes in $[Ca^{2+}]_m$. Mitochondria are main cellular calcium stores and play a crucial role for cellular calcium homeostasis. Mitochondria maintain intra-organelle calcium homeostasis by continuously precipitating the $[Ca^{2+}]_m$ to the non-ionized calcium stores, the matrix electron-dense granules, and releasing Ca^{2+} from the granules [17–19, 35, 46–48]. Drugs, hormones, or pathological conditions alter intramitochondrial calcium homeostasis in favor of $[Ca^{2+}]_m$ or non-ionized calcium granules [18, 19, 46, 47, 49]. Increased Ca^{2+} is a prominent feature in the tissues from patients with Alzheimer's disease, Parkinson's disease, Huntington's disease, and amyotro-

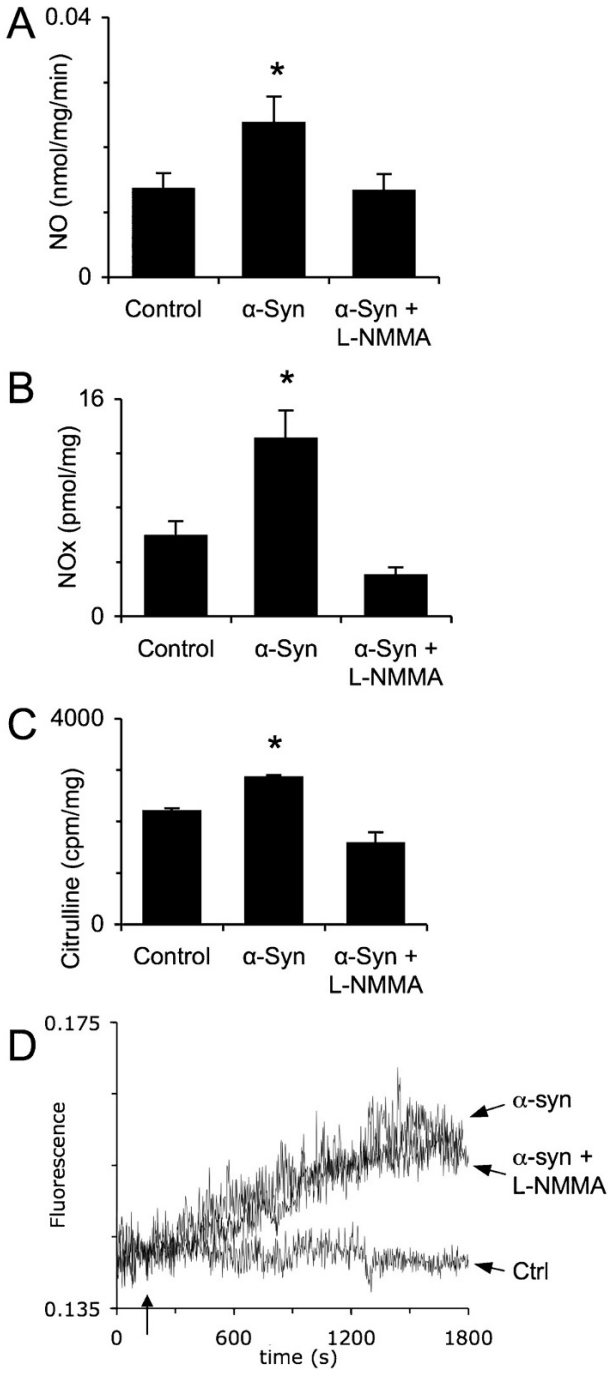

Figure 7. α-Syn stimulates mtNOS and increases $[Ca^{2+}]_m$ in isolated mitochondria. mtNOS activity of isolated brain mitochondria treated with un-aggregated α-syn (Control), aggregated α-syn (α-syn), or aggregated α-syn upon pretreatment with L-NMMA (α-syn + L-NMMA). (*A*) mtNOS activity measured by oxyhemoglobin assay and expressed as nmol NO per mg mitochondrial protein per minute. (*B*) mtNOS activity determined by chemiluminescence assay and expressed as pmol NOx per mg mitochondrial protein. (*C*) mtNOS activity determined by radioassay and expressed as cpm L-citrulline per mg mitochondrial protein. (*D*) Real-time determination of $[Ca^{2+}]_m$ in mitochondria treated with un-aggregated α-syn (Ctrl), aggregated α-syn (α-syn), or aggregated α-syn when mitochondria were pretreated with L-NMMA (α-syn + L-NMMA). *$p<0.05$ compared with the control.

phic lateral sclerosis [50]. While Ca^{2+} regulates several physiological processes, excess Ca^{2+} initiates apoptosis *via* mitochondrial pathway [51]. Under stressed conditions, Ca^{2+} is released from mitochondria, which induces cellular damage and ultimately cell death. Although the exact mechanism of intramitochondrial calcium homeostasis is not fully understood, our previous studies demonstrated that oxidative stress in mitochondria of human cancer cells [19] and rat heart [35] induces release of Ca^{2+} from non-ionized stores. Several apoptosis-inducing agents causes cytochrome *c* release by elevating $[Ca^{2+}]_m$ in cancer cells [19]. Likewise, amyloid β causes neuronal apoptosis by elevating $[Ca^{2+}]_m$ [52]. Elevated $[Ca^{2+}]_m$ also accounts for mtNOS stimulation leading to oxidative stress and cytochrome *c* release in heart mitochondria undergoing ischemia/reperfusion [35]. Figure 4 shows that wild-type or A53T α-syn increased $[Ca^{2+}]_m$ compared to control cells. Mitochondrial Ca^{2+} is sensitive to protonophores such as FCCP. As shown, FCCP almost completely abolished the $[Ca^{2+}]_m$ signals. Ionomycin, a Ca^{2+} ionophore that elevates cytosolic and $[Ca^{2+}]_m$ [25] was used as a positive control. As shown in Figure 4, ionomycin caused a significant increase in $[Ca^{2+}]_m$, validating the sensitivity of the fluorescence assay used in the present study. As to other potentially important consequences of the $[Ca^{2+}]_m$-mediated mitochondrial dysfunction, the increase in $[Ca^{2+}]_m$-sensitive mitochondrial NO may be critical for neuronal cells.

Overexpression of A53T or A30P mutant α-syn in human embryonic kidney (HEK) cells exhibits greater toxicity than the wild-type [53]. Our findings show that in human neuroblastoma SHSY cells toxicity caused by overexpression of A53T is comparable to that of wild-type α-syn. Similar toxicities of A53 and wild-type α-syn might be due to high level of overexpression reached in the present study, or indicate that α-syn toxicity is cell-type specific.

To confirm our findings in SHSY cells overexpressing wild-type or A53T mutant α-syn, we performed studies on isolated mitochondria treated with aggregated or unaggregated α-syn. First, aggregation of α-syn was tested. Figure 5C shows α-syn monomer forms aggregated oligomers, which is consistent with an earlier observation [9]. To test the association of α-syn with mitochondria, the present study tested bindings of aggregated and unaggregated α-syn to isolated mitochondria. Figure 5D shows that aggregated α-syn associated with mitochondria, whereas unaggregated α-syn shows minimal association with mitochondria and largely remains in the supernatant. Figure 5E shows that aggregated α-syn associated with mitochondrial membrane was resistant to removal by proteinase K, whereas un-aggregated α-syn was fully

removed when mitochondria were treated with proteinase K. Proteinase K removes proteins that unspecifically associate with the surface of mitochondrial outer membrane [33, 54]. Figure 5F shows that aggregated α-syn does not associate with microsomes, further suggesting specific association of α-syn with mitochondria. Thus, novel findings presented under Figure 5 strongly indicate that aggregated α-syn specifically associated with the mitochondria.

The interaction of aggregated α-syn with mitochondria and understanding consequence of this interaction could provide important insights into the mechanism of cell death caused by α-syn. α-Syn induces apoptosis *via* mitochondria-dependent pathways downstream to cytochrome *c* release, including caspases activation [55]. Figure 6A shows that aggregated α-syn that associates with isolated mitochondria (Fig. 5D) caused release of cytochrome *c*. Cytochrome *c* is a mediator of apoptotic cell death involved in α-syn-induced oxidative stress in Parkinson's disease and related disorders [37, 56]. Other proteins involved in neurodegenerative diseases including amyloid β peptide [20, 57] and Huntingitin [58] cause release of cytochrome *c*. Thus, the novel findings presented in Figure 6A confirm results of Figure 2 of overexpressed wild-type or A53T α-syn and suggest that cytochrome *c* release may account for apoptosis induced by α-syn.

Nitrated synuclein inclusions with degenerating mitochondria in cell bodies [39] indicate involvement of peroxynitrite in pathological effects of α-syn. Protein tyrosine nitration that is a reliable marker of peroxynitrite is increased in neurons undergoing α-syn-induced apoptosis [11]. In dopaminergic neurons of *Nurr1*-knockdown mice, a model for Parkinson's disease, increased tyrosine nitration and cytochrome *c* release occur along with increased cytoplasmic NOS activity [59]. Figure 6B shows aggregated α-syn increased tyrosine nitration of mitochondrial proteins, strongly suggesting that aggregated α-syn increased mitochondrial peroxynitrite. Increased LPO, an indicator of oxidative stress,was seen in neurons overexpressing α-syn [11] and in the substantia nigra of patients with Parkinson's disease [60]. Figure 6C shows that aggregated α-syn increased LPO of isolated brain mitochondria, indicating aggregated α-syn elevated oxidant radicals in the mitochondria. PTP opening is a marker of oxidative stress and apoptosis [61]. In some cases, PTP, which is associated with the opening of the mitochondrial megapore, may be implicated in the release of cytochrome *c* [62]. Figure 6D shows that aggregated α-syn induced PTP opening in isolated mitochondria. Findings presented in Figures 6A–D indicate that interaction of aggregated α-syn with mitochondria induced mitochondrial hallmarks of oxidative stress and apoptosis. Figures 6A–C also show that α-syn-induced cytochrome *c* release, increased protein tyrosine nitration and LPO were prevented by inhibition of mtNOS activity. Stimulation of mtNOS in mitochondria isolated from rat heart [35] or liver [17], or human breast cells [19] causes cytochrome *c* release, elevates protein tyrosine nitration and LPO, and decreases transmembrane potential [16]. Findings presented in Figures 6A–C suggest that mtNOS is involved in effects of α-syn on brain mitochondria. Thus, we tested whether α-syn increases mtNOS activity. Figures 7A–C show that aggregated α-syn stimulated mtNOS activity of isolated brain mitochondria, and that L-NMMA inhibited this effect of α-syn. Figure 7 confirms data obtained from cell experiments and shows a dramatic increase in the mitochondrial NO of mitochondria with aggregated α-syn compared to un-aggregated α-syn.

mtNOS is Ca^{2+} sensitive and elevation of $[Ca^{2+}]_m$ stimulates mtNOS activity [17–19, 63–66]. Mitochondrial calcium homeostasis in cell systems comprises exchange of calcium with cytoplasm and intramitochondrial homeostasis. Figure 4A shows that overexpressing α-syn wild-type or A53T increases $[Ca^{2+}]_m$ in SHSY cells. To study whether elevated $[Ca^{2+}]_m$ shown in Figure 4A was due to increased Ca^{2+} efflux into mitochondria or release of Ca^{2+} from intramitochondrial granules, the direct effect of α-syn on isolated mitochondria was tested. Figure 7D shows that aggregated α-syn, indeed, increased $[Ca^{2+}]_m$. Thus, this could serves the mechanism underlying stimulation of mtNOS by α-syn. As shown, α-syn-induced increase in $[Ca^{2+}]_m$ was not sensitive to L-NMMA. Findings in the present study suggest that aggregated α-syn interacted with mitochondria, which increased $[Ca^{2+}]_m$ by shifting the balance between $[Ca^{2+}]_m$ and matrix granules in the favor of $[Ca^{2+}]_m$. Elevated $[Ca^{2+}]_m$ stimulated mtNOS activity that increased mitochondrial peroxynitrite, caused oxidative modification of mitochondrial proteins and membranes, and released cytochrome *c* from the mitochondria. We have also shown that L-NMMA inhibited α-syn-induced mtNOS stimulation, whereas it did not affect $[Ca^{2+}]_m$. This finding indicates that effect of L-NMMA on inhibiting effects of α-syn was due to inhibition of mtNOS.

Taken together, the present study reveals the mitochondrial localization of α-syn. Overexpressing wild-type or A53T mutant α-syn in SHSY cells or treating isolated mitochondria with aggregated α-syn induce cytochrome *c* release from mitochondria and increase mitochondrial oxidative stress. Findings presented here indicate the significance of mitochondria in oxidative stress and apoptosis induced by α-syn. The

present study also suggests a novel role for mtNOS in cytochrome *c* release and oxidative stress induced by α-syn.

Acknowledgements. We thank Dr. Julia M. George for generously providing the monoclonal antibody (H3C). Financial support was provided by the National Institute on Aging (award AG023264–02) and American Heart Association (award 0565221B). We thank Dr. Nazarewicz for assist with chemiluminescence measurements.

1 Giasson, B. I., Duda, J. E., Murray, I. V., Chen, Q., Souza, J. M., Hurtig, H. I., Ischiropoulos, H., Trojanowski, J. Q. and Lee, V. M. (2000) Oxidative damage linked to neurodegeneration by selective alpha-synuclein nitration in synucleinopathy lesions. Science 290, 985–989.
2 Masliah, E., Rockenstein, E., Veinbergs, I., Mallory, M., Hashimoto, M., Takeda, A., Sagara, Y., Sisk, A. and Mucke, L. (2000) Dopaminergic loss and inclusion body formation in alpha-synuclein mice: Implications for neurodegenerative disorders. Science 287, 1265–1269.
3 Periquet, M., Fulga, T., Myllykangas, L., Schlossmacher, M. G. and Feany, M. B. (2007) Aggregated alpha-synuclein mediates dopaminergic neurotoxicity *in vivo*. J. Neurosci. 27, 3338–3346.
4 Conway, K. A., Harper, J. D. and Lansbury, P. T. (1998) Accelerated *in vitro* fibril formation by a mutant alpha-synuclein linked to early-onset Parkinson disease. Nat. Med. 4, 1318–1320.
5 Biere, A. L., Wood, S. J., Wypych, J., Steavenson, S., Jiang, Y., Anafi, D., Jacobsen, F. W., Jarosinski, M. A., Wu, G. M., Louis, J. C., Martin, F., Narhi, L. O. and Citron, M. (2000) Parkinson's disease-associated alpha-synuclein is more fibrillogenic than beta- and gamma-synuclein and cannot cross-seed its homologs. J. Biol. Chem. 275, 34574–34579.
6 Kruger, R., Kuhn, W., Muller, T., Woitalla, D., Graeber, M., Kosel, S., Przuntek, H., Epplen, J. T., Schols, L. and Riess, O. (1998) Ala30Pro mutation in the gene encoding alpha-synuclein in Parkinson's disease. Nat. Genet. 18, 106–108.
7 Munoz, E., Oliva, R., Obach, V., Marti, M. J., Pastor, P., Ballesta, F. and Tolosa, E. (1997) Identification of Spanish familial Parkinson's disease and screening for the Ala53Thr mutation of the alpha-synuclein gene in early onset patients. Neurosci. Lett. 235, 57–60.
8 Polymeropoulos, M. H., Lavedan, C., Leroy, E., Ide, S. E., Dehejia, A., Dutra, A., Pike, B., Root, H., Rubenstein, J., Boyer, R., Stenroos, E. S., Chandrasekharappa, S., Athanassiadou, A., Papapetropoulos, T., Johnson, W. G., Lazzarini, A. M., Duvoisin, R. C., Di Iorio, G., Golbe, L. I. and Nussbaum, R. L. (1997) Mutation in the alpha-synuclein gene identified in families with Parkinson's disease. Science 276, 2045–2047.
9 Ding, T. T., Lee, S. J., Rochet, J. C. and Lansbury, P. T. Jr. (2002) Annular alpha-synuclein protofibrils are produced when spherical protofibrils are incubated in solution or bound to brain-derived membranes. Biochemistry 41, 10209–10217.
10 Hsu, L. J., Sagara, Y., Arroyo, A., Rockenstein, E., Sisk, A., Mallory, M., Wong, J., Takenouchi, T., Hashimoto, M. and Masliah, E. (2000) Alpha-synuclein promotes mitochondrial deficit and oxidative stress. Am. J. Pathol. 157, 401–410.
11 Lee, M., Hyun, D., Halliwell, B. and Jenner, P. (2001) Effect of the overexpression of wild-type or mutant alpha-synuclein on cell susceptibility to insult. J. Neurochem. 76, 998–1009.
12 Abou-Sleiman, P. M., Muqit, M. M. and Wood, N. W. (2006) Expanding insights of mitochondrial dysfunction in Parkinson's disease. Nat. Rev. Neurosci. 7, 207–219.
13 Hasegawa, T., Matsuzaki-Kobayashi, M., Takeda, A., Sugeno, N., Kikuchi, A., Furukawa, K., Perry, G., Smith, M. A. and Itoyama, Y. (2006) Alpha-synuclein facilitates the toxicity of oxidized catechol metabolites: Implications for selective neurodegeneration in Parkinson's disease. FEBS Lett. 580, 2147–2152.
14 Ved, R., Saha, S., Westlund, B., Perier, C., Burnam, L., Sluder, A., Hoener, M., Rodrigues, C. M., Alfonso, A., Steer, C., Liu, L., Przedborski, S. and Wolozin, B. (2005) Similar patterns of mitochondrial vulnerability and rescue induced by genetic modification of alpha-synuclein, parkin, and DJ-1 in *Caenorhabditis elegans*. J. Biol. Chem. 280, 42655–42668.
15 Zhou, Z. D., Yap, B. P., Gung, A. Y., Leong, S. M., Ang, S. T. and Lim, T. M. (2006) Dopamine-related and caspase-independent apoptosis in dopaminergic neurons induced by overexpression of human wild type or mutant alpha-synuclein. Exp. Cell Res. 312, 156–170.
16 Ghafourifar, P. and Cadenas, E. (2005) Mitochondrial nitric oxide synthase. Trends Pharmacol. Sci. 26, 190–195.
17 Ghafourifar, P., Schenk, U., Klein, S. D. and Richter, C. (1999) Mitochondrial nitric-oxide synthase stimulation causes cytochrome c release from isolated mitochondria. Evidence for intramitochondrial peroxynitrite formation. J. Biol. Chem. 274, 31185–31188.
18 Nazarewicz, R. R., Zenebe, W. J., Parihar, A., Parihar, M. S., Voccaro, M. and Ghafourifar P. (2007) 12(S)-Hydroperoxyeicosatetraenoic acid (12-HETE) increases nitric oxide formation in mitochondria by increasing intramitochondrial ionized calcium. Arch. Biochem. Biophys. 468, 114–120.
19 Nazarewicz, R. R., Zenebe, W. J., Parihar, A., Larson, S. K., Alidema, E., Choi, J. and Ghafourifar, P. (2007) Tamoxifen induces oxidative stress and mitochondrial apoptosis *via* stimulating mitochondrial nitric oxide synthase. Cancer Res. 67, 1282–1290.
20 Kim, H. S., Lee, J. H., Lee, J. P., Kim, E. M., Chang, K. A., Park, C. H., Jeong, S. J., Wittendorp, M. C., Seo, J. H., Choi, S. H. and Suh, Y. H. (2002) Amyloid beta peptide induces cytochrome C release from isolated mitochondria. Neuroreport 13, 1989–1993.
21 Manczak, M., Anekonda, T. S., Henson, E., Park, B. S., Quinn, J. and Reddy, P. H. (2006) Mitochondria are a direct site of A beta accumulation in Alzheimer's disease neurons: Implications for free radical generation and oxidative damage in disease progression. Hum. Mol. Genet. 15, 1437–1449.
22 Choo, Y. S., Johnson, G. V., MacDonald, M., Detloff, P. J. and Lesort, M. (2004) Mutant huntingtin directly increases susceptibility of mitochondria to the calcium-induced permeability transition and cytochrome c release. Hum. Mol. Genet. 13, 1407–1420.
23 Hashimoto, M., Yoshimoto, M., Sisk, A., Hsu, L. J., Sundsmo, M., Kittel, A., Saitoh, T., Miller, A. and Masliah, E. (1997) NACP, a synaptic protein involved in Alzheimer's disease, is differentially regulated during megakaryocyte differentiation. Biochem. Biophys. Res. Commun. 237, 611–616.
24 Marks, J. D., Boriboun, C. and Wang, J. (2005) Mitochondrial nitric oxide mediates decreased vulnerability of hippocampal neurons from immature animals to NMDA. J. Neurosci. 25, 6561–6575.
25 Yi, M., Weaver, D. and Hajnoczky, G. (2004) Control of mitochondrial motility and distribution by the calcium signal: A homeostatic circuit. J. Cell Biol. 167, 661–672.
26 Lopez-Perez, M. J. (1994) Preparation of synaptosomes and mitochondria from mammalian brain. Methods Enzymol. 228, 403–411.
27 Wykle, R. L. and Schremmer, J. M. (1974) A lysophospholipase D pathway in the metabolism of ether-linked lipids in brain microsomes. J. Biol. Chem. 249, 1742–1746.
28 Ghafourifar, P., Asbury, M. L., Joshi, S. S. and Kincaid, E. D. (2005) Determination of mitochondrial nitric oxide synthase activity. Methods Enzymol. 396, 424–444.
29 Almeida, A. and Medina, J. M, (1998) A rapid method for the isolation of metabolically active mitochondria from rat neurons and astrocytes in primary culture. Brain Res. Brain Res. Protoc. 2, 209–214.

30 Zhang, W., Wang, T., Pei, Z., Miller, D. S., Wu, X., Block, M. L., Wilson, B., Zhang, W., Zhou, Y., Hong, J. S. and Zhang, J. (2005) Aggregated alpha-synuclein activates microglia: A process leading to disease progression in Parkinson's disease. FASEB J. 19, 533–542.
31 Fink, A. L. (2006) The aggregation and fibrillation of alpha-synuclein. Acc. Chem. Res. 39, 628–634.
32 Ghafourifar, P., Klein, S. D., Schucht, O., Schenk, U., Pruschy, M., Rocha, S. and Richter, C. (1999) Ceramide induces cytochrome c release from isolated mitochondria. Importance of mitochondrial redox state. J. Biol. Chem. 274, 6080–6084.
33 Gao, S., Chen, J., Brodsky, S. V., Huang, H., Adler, S., Lee, J. H., Dhadwal, N., Cohen-Gould, L., Gross, S. S. and Goligorsky, M. S. (2004) Docking of endothelial nitric oxide synthase (eNOS) to the mitochondrial outer membrane: A pentabasic amino acid sequence in the autoinhibitory domain of eNOS targets a proteinase K-cleavable peptide on the cytoplasmic face of mitochondria. J. Biol. Chem. 279, 15968–15974.
34 Panov, A., Dikalov, S., Shalbuyeva, N., Hemendinger, R., Greenamyre, J. T. and Rosenfeld, J. (2007) Species- and tissue-specific relationships between mitochondrial permeability transition and generation of ROS in brain and liver mitochondria of rats and mice. Am. J. Physiol. Cell Physiol. 292, C708-C718.
35 Zenebe, W. J., Nazarewicz, R. R., Parihar, M. S. and Ghafourifar, P. (2007) Hypoxia/reoxygenation of isolated rat heart mitochondria causes cytochrome c release and oxidative stress; evidence for involvement of mitochondrial nitric oxide synthase. J. Mol. Cell Cardiol. 43, 411–419.
36 Smith, W. W., Jiang, H., Pei, Z., Tanaka, Y., Morita, H., Sawa, A., Dawson, V. L., Dawson, T. M. and Ross, C. A. (2005) Endoplasmic reticulum stress and mitochondrial cell death pathways mediate A53T mutant alpha-synuclein-induced toxicity. Hum. Mol. Genet. 14, 3801–3811.
37 Volles, M. J. and Lansbury, P. T. Jr. (2007) Relationships between the sequence of alpha-synuclein and its membrane affinity, fibrillization propensity, and yeast toxicity. J. Mol. Biol. 366, 1510–1522.
38 Perier, C., Bove, J., Wu, D. C., Dehay, B., Choi, D. K., Jackson-Lewis, V., Rathke-Hartlieb, S., Bouillet, P., Strasser, A., Schulz, J. B., Przedborski, S. and Vila, M. (2007) Two molecular pathways initiate mitochondria-dependent dopaminergic neurodegeneration in experimental Parkinson's disease. Proc. Natl. Acad. Sci. USA 104, 8161–8166.
39 Martin, L. J., Pan, Y., Price, A. C., Sterling, W., Copeland, N. G., Jenkins, N. A., Price, D. L. and Lee, M. K. (2006) Parkinson's disease alpha-synuclein transgenic mice develop neuronal mitochondrial degeneration and cell death. J. Neurosci. 26, 41–50.
40 Li, W. W., Yang, R., Guo, J. C., Ren, H. M., Zha, X. L., Cheng, J. S. and Cai, D. F. (2007) Localization of alpha-synuclein to mitochondria within midbrain of mice. Neuroreport 18, 1543–1546.
41 Giasson, B. I., Duda, J. E., Quinn, S. M., Zhang, B., Trojanowski, J. Q. and Lee, V. M. (2002) Neuronal alpha-synucleinopathy with severe movement disorder in mice expressing A53T human alpha-synuclein. Neuron 34, 521–533.
42 McLean, P. J., Kawamata, H., Ribich, S. and Hyman, B. T. (2000) Membrane association and protein conformation of alpha-synuclein in intact neurons. Effect of Parkinson's disease-linked mutations. J. Biol. Chem. 275, 8812–8816.
43 Shults, C. W. (2006) Lewy bodies. Proc. Natl. Acad. Sci. USA 103, 1661–1668.
44 Beal, M. F. (1998) Excitotoxicity and nitric oxide in Parkinson's disease pathogenesis. Ann. Neurol. 44, S110-S114.
45 Pacher, P., Beckman, J. S. and Liaudet, L. (2007) Nitric oxide and peroxynitrite in health and disease. Physiol. Rev. 87, 315–424.
46 Ashraf, M. and Bloor, C. M. (1976) X-ray microanalysis of mitochondrial deposits in ischemic myocardium. Virchows Arch. B Cell Pathol. 22, 287–297.
47 Pinton, P., Leo, S., Wieckowski, M. R., Di Benedetto, G. and Rizzuto, R. (2004) Long-term modulation of mitochondrial Ca^{2+} signals by protein kinase C isozymes. J. Cell Biol. 165, 223–232.
48 Parducz, A. and Joo, F. (1976) Visualization of stimulated nerve endings by preferential calcium accumulation of mitochondria. J. Cell Biol. 69, 513–517.
49 Karcsu, S., Laszlo, F. A., Jancso, G., Toth, L. and Bacsy, E. (1982) Morphological evidence for the involvement of calcium in neurohypophysial hormone release. Brain Res. 238, 278–281.
50 Mattson, M. P. (2007) Calcium and neurodegeneration. Aging Cell 6, 337–350.
51 Mattson, M. P. and Chan, S. L. (2003) Calcium orchestrates apoptosis. *Nat. Cell Biol.* 5, 1041–1043.
52 Begley, J. G., Duan, W., Chan, S., Duff, K. and Mattson, M. P. (1999) Altered calcium homeostasis and mitochondrial dysfunction in cortical synaptic compartments of presenilin-1 mutant mice. J. Neurochem. 72, 1030–1039.
53 Ostrerova, N., Petrucelli, L., Farrer, M., Mehta, N., Choi, P., Hardy, J. and Wolozin, B. (1999) Alpha-synuclein shares physical and functional homology with 14–3-3 proteins. J. Neurosci. 19, 5782–5791.
54 Diekert, K., Kispal, G., Guiard, B. and Lill, R. (1999) An internal targeting signal directing proteins into the mitochondrial intermembrane space. Proc. Natl. Acad. Sci. USA 96, 11752–11757.
55 Seo, J. H., Rah, J. C., Choi, S. H., Shin, J. K., Min, K., Kim, H. S., Park, C. H., Kim, S., Kim, E. M., Lee, S. H., Lee, S., Suh, S. W. and Suh, Y. H. (2002) Alpha-synuclein regulates neuronal survival *via* Bcl-2 family expression and PI3/Akt kinase pathway. FASEB J. 16, 1826–1828.
56 Hashimoto, M., Takeda, A., Hsu, L. J., Takenouchi, T. and Masliah, E. (1999) Role of cytochrome c as a stimulator of alpha-synuclein aggregation in Lewy body disease. J. Biol. Chem. 274, 28849–28852.
57 Chen, S., Lee, J. M., Zeng, C., Chen, H., Hsu, C. Y. and Xu, J. (2006) Amyloid beta peptide increases DP5 expression *via* activation of neutral sphingomyelinase and JNK in oligodendrocytes. J. Neurochem. 97, 631–640.
58 Wang, X., Zhu, S., Drozda, M., Zhang, W., Stavrovskaya, I. G., Cattaneo, E., Ferrante, R. J., Kristal, B. S. and Friedlander, R. M. (2003) Minocycline inhibits caspase-independent and -dependent mitochondrial cell death pathways in models of Huntington's disease. Proc. Natl. Acad. Sci. USA 100, 10483–10487.
59 Imam, S. Z., Jankovic, J., Ali, S. F., Skinner, J. T., Xie, W., Conneely, O. M. and Le, W. D. (2005) Nitric oxide mediates increased susceptibility to dopaminergic damage in Nurr1 heterozygous mice. FASEB J. 19, 1441–1450.
60 Jenner, P. and Olanow, C. W. (1998) Understanding cell death in Parkinson's disease. Ann. Neurol. 44, S72-S84.
61 Kroemer, G., Galluzzi, L. and Brenner, C. (2007) Mitochondrial membrane permeabilization in cell death. Physiol. Rev. 87, 99–163.
62 Bernardi, P. and Petronilli, V. (1996) The permeability transition pore as a mitochondrial calcium release channel: A critical appraisal. J. Bioenerg. Biomembr. 28, 131–138.
63 Alvarez, S., Valdez, L. B., Zaobornyj, T. and Boveris, A. (2003) Oxygen dependence of mitochondrial nitric oxide synthase activity. Biochem. Biophys. Res. Commun. 305, 771–775.
64 Ghafourifar, P. and Richter, C. (1997) Nitric oxide synthase activity in mitochondria. FEBS Lett. 418, 291–296.
65 Arnaiz, S. L., D'Amico, G., Paglia, N., Arismendi, M., Basso, N. and Rosario, Lores, A. M. (2004) Enriched environment, nitric oxide production and synaptic plasticity prevent the aging-dependent impairment of spatial cognition. Mol. Aspects Med. 25, 91–101.
66 Lores-Arnaiz, S., D'Amico, G., Czerniczyniec, A., Bustamante, J. and Boveris, A. (2004) Brain mitochondrial nitric oxide synthase: *In vitro* and *in vivo* inhibition by chlorpromazine. Arch. Biochem. Biophys. 430, 170–177.